

## **Thickness Determination of the Silica Sand Deposits by Using Ground Penetrating Radar (GPR) and Multichannel Analysis of Surface Waves (MASW) Geophysical Techniques**

Dr Ibrahim E. Ahmed Amari<sup>1</sup>, Ghassan S. Alsulaimani<sup>1</sup>, Usman Pervaiz<sup>2</sup>

<sup>1</sup>*Department Of Geology & Geography, Georgia Southern University, Statesboro. Georgia, USA*

<sup>1</sup>*Department Of Geosciences, Missouri University Of Science & Technology, Rolla. Missouri, USA*

<sup>2</sup>*Department Of Civil And Environmental Engineering, Hanyang University, Seoul, South Korea*

**Abstract:** This paper summarizes using geophysical methods for the geomorphological characterization of subsurface features has numerous advantages over traditional exploration methods, because of their noninvasive and rapid nature. In this study, we compared the results of two geophysical methods with each other. We also discuss their possibilities and limitations in a geomorphological investigation. Ground penetrating radar (GPR) and multichannel analysis of surface waves (MASW) methods were applied at silica sand in southern Dawmat Al Jandal, Al Jawf in Saudi Arabia. By combining these methods, we were able to estimate the thickness of the sand deposits and to better understand depositional environments under the same conditions.

During the course of these investigations, the authors tried to review the acquired 1620 meters of ground penetrating radar (GPR) data to image internal reflections (if any) within the sand and the top of the underlying sandstone; 27 MASW field records were acquired at particular location, which generated 1-D and 2-D shear wave velocity profiles. Core samples obtained from drilling were used to validate the findings of both geophysics methods.

The results concluded that the both of the geophysical investigation techniques were successful and proved to be useful methods for the exploration of shallow subsurface areas. The results were equal to or slightly different from the corresponding core holes' measurements.

### **I. INTRODUCTION**

Geophysical applications have shown significant growth in recent years after gaining enormous acceptance in fields of geological, geotechnical, and in the mining (Annan, 2002; Pellerin, 2002; Burger et al., 2006). These techniques generally applied to obtain detailed near surface information in terms of layers thickness, economic mineral deposits, depth of bedrock and lithology. Geophysical investigations are an excellent alternative to the conventional core hole methods to provide information of 1-D or 2-D, easy field acquisition, processing and interpenetrations. These tasks can be performed by using the principles of electromagnetic radiation pulses and seismic acoustical wave's propagation that are sent out at predetermined distances for data acquisition, processing, and interpretation. These kinds of investigations are generally limited at shallower depths, especially less than 30 meters. The geophysical techniques applied for this study include; ground penetrating radar (GPR), multichannel analysis of surface waves (MASW). The results were validated with the drilled cores holes observations and both of these methods showed satisfactory correlation with the core holes measurements.

GPR provides detailed information about the subsurface such as the geological structures, folds, strata sequences, utilities, tombs, ancient graves, landmines, and it estimates the thickness of different earth materials, such as soils (Reynolds, 1997; Kovic and Anderson et al., 2005) which are site-dependent. The GPR data is recorded digitally and requires extensive post-acquisition processing, that can be done either in the field or in the office. There are many different GPR processing and analysis techniques (Cassidy, 2009). However, the core point data quality is more reliable in subsurface investigations.

Multichannel Analysis of Surface Waves (MASW) is a relatively new geophysical method that was first introduced to the industry by the Kansas Geological Survey in the beginning of this century (Park et al., 1999; Xia et al., 1999). It applies the relationship between surface waves and shear waves to ultimately generate a shear wave velocity profile of the subsurface. The MASW method involves the inversion of a wave that has sampled an area nearly as wide as it is deep, which provides a smoothed and smeared version of what really exists in the subsurface (Xia, et al., 2001). It has been commonly applied in mining exploration to determine the depths and thicknesses of the geological strata at a potential mine site. It may also be applied on much smaller scales in the transportation industry to identify damaged areas on asphalt or concrete pavements with high resolution" (Anderson, 2010). The main advantages of the MASW seismic technique is the strength of the utilized surface wave, much greater than the other wave forms; therefore surface waves are more discernable in

the presence of noise. In a record presenting good signal to noise (S/N) ratio, the signal strength of the surface wave should be evident by the linear sloping features of the dispersive wave forms. Surface waves, on an active shot record, are often identified by the smooth sloping behavior as the wave travels down the geophone array (Ivanov, Park and Xia 2009). The linear slope represents the phase velocity of the particular surface wave, and can be used to transform the shot record data into a dispersion curve, relating phase velocity to wave frequency (Park et al. 2000).

Unconfined Economic Value is one of the primary parameters by which Silica sands are evaluated for their usefulness as manufacturing materials. The unconfined Silica rate of sand is known to be controlled by such factors as depositional environment, transportation routes, bedding orientation, presence of micro fractures, and petrographic characteristics (grain size, grain shape, matrix-cement mineralogy, etc.). Unconfined Economic Value is one of the primary parameters by which Silica sands are evaluated for their usefulness as manufacturing materials and demand increased quantities and higher purity, which may bring synthetic silica into play; such as manufacturing glass, foundry sand, fracturing, filtration, abrasives, silicon carbide, filler, silica brick, and sodium silicate. The unconfined Silica rate of sand is known to be controlled by such factors as depositional environment, transportation routes, bedding orientation, presence of micro fractures, and petrographic characteristics (grain size, grain shape, matrix-cement mineralogy, etc.). This study considered being the first type of investigation using geophysical applications in the region. The attempts were made to compare results between geophysical tools and core holes data on silica sand deposits in southern Dawmat Al Jandal, Al Jawf in Saudi Arabia.

## II. OVERVIEW OF THE STUDY AREA

In Saudi Arabia the siliceous material and sandstone most commonly belong to Paleozoic, Mesozoic, and Cenozoic ages that limit the Arabian shield surrounded by the north, east, and south. The silica sand deposits of upper part Sirhan Formation are located about 44 km to the south of Dawmat Al Jandal town (Bramkamp et al., 1963). The Sirhan Formation is described as a Tertiary unit, mainly composed of white sands, characterized by small hills (with varying thickness of 10 - 40 m) and underlying slightly consolidated sandstone (see Figures 1). The Sirhan Formation sands and sandstones with having total thickness of 100m are believed to be Miocene and perhaps partly Pliocene in age (Bramkamp et al., 1963). Through geological processes of transportation, resedimentation, and erosion lead to purification of the sand and the expulsion of material less stable.

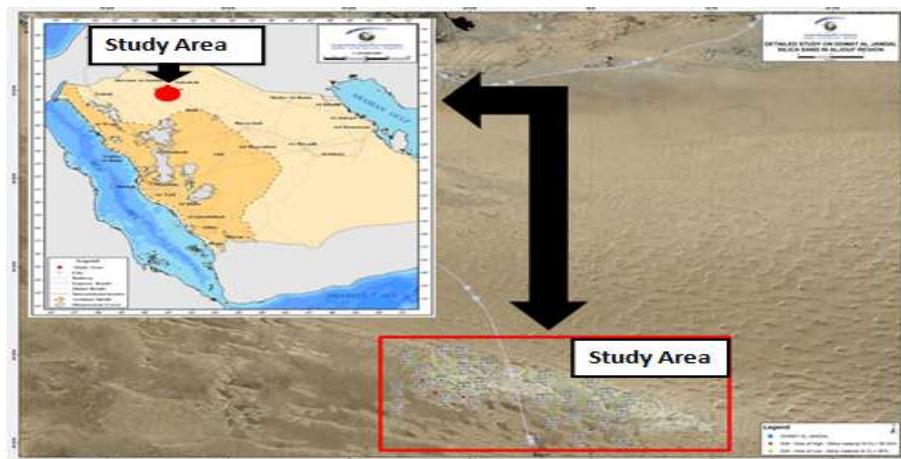


**Figure 1.** Location Map of the Study Area.

The sand deposits consist predominantly of well-sorted white silica sands covering an area of about 20 km<sup>2</sup>. The average thickness of sands in the study area was found 20 m. On the basis of drilling results, the average thickness of silica sand as 16m and total estimated reserve is about 160 million tons. The source of silica sands is predominantly quartz with the following average contents: silica 97%, iron oxide 0.2%, and alumina 1.4% (see Figure 2). Sands are fine- to coarse-grained and moderately-well sorted. Quartz particles are sub-rounded to sub-angular. The bedding planes observed within the sandstone sequence were apparent and graded horizons that indicate the deposition from multi sedimentary cycles. Finally, through geological processes of transport, resedimentation, and erosion lead to purification of the sand and the expulsion of material less stable and thus, that we get the high purity sand. (see outcrop in Figure 3). The unit displays regular vertical joints and fractures without filling materials.

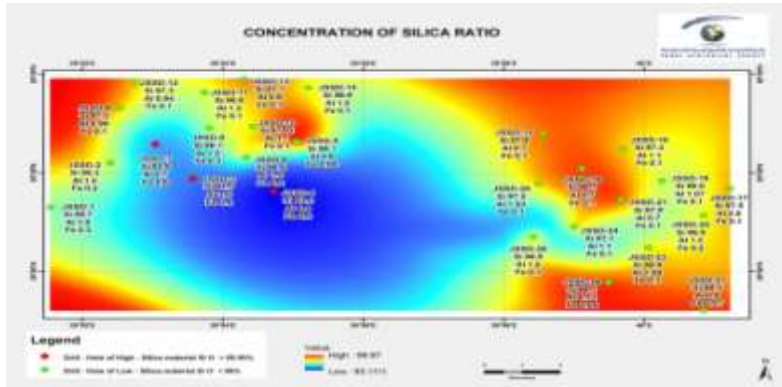


**Figure 2.** Silica concentration in the study area at different locations (After Ghandoura et al., 2012)



**Figure 3.** White Silica Sand Outcrop of the Sirhan Formation (photo by the authors).

### III. METHODOLOGY

#### 3.1 Ground Penetrating Radar (GPR)

Ground penetrating radar (GPR) is a subsurface geophysical exploration tool that involves the transmission of microwave range electromagnetic radiation into the subsurface and the recording of the arrival times and magnitudes of energy that is reflected from features or interfaces in the subsurface (Jol and Smith, 1991). The typical application of GPR involves a pair of transmitting and receiving dipole antennas in common-offset mode that are moved across the surface to generate 2D cross-sections of the subsurface (see Figure4).

In summary, ground penetrating radar data was acquired at the sites. Unfortunately, the lower frequency GPR antenna was able to image the subsurface to depths of only 20 meters. As a consequence, the top of the bedrock in the study areas could not be mapped using this technique.

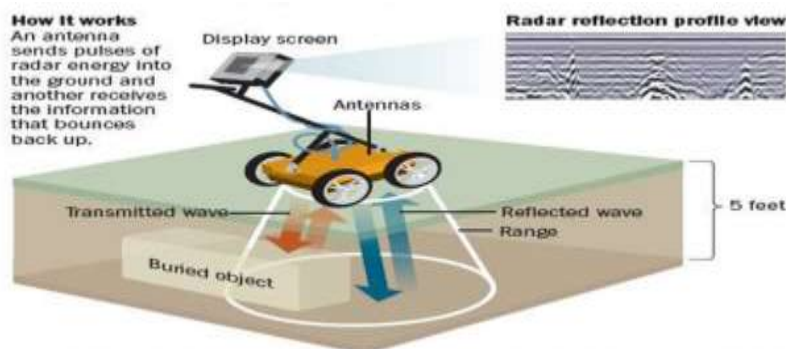


**Figure 4.** Simple diagram shows the basic components of GPR System

The radar data were acquired using the SIR-3000 ground penetrating radar instrument which can be used on the ground's surface or in core holes. The antennae with operating frequencies of 100 and 200 MHz were chosen for measurements of the resolution and the penetrating depth thickness of the silica sand deposits (Figure 5). Studies were conducted at twenty-seven selected sites. A total of 1620 linear meters of ground penetrating radar (GPR) data were collected across the tape that was stretched 30 meters each time. The measurements were taken against the profile distance and each recording (trace) associated with the depth below

the surface. The measured microwave radar propagation velocity correlates well to the root of the material constant. With a good estimate of the propagation velocity, images with respect to travel time (two-way travel time down and the time needed to return to the surface) can be transformed directly to respective output images with depth. The GPR data was recorded digitally and processed by using core point analysis techniques (Cassidy, 2009a) by using RADANTM (Radar Data Analyzer) software package, prepared by Geophysical Survey Systems Inc. (GSSI).

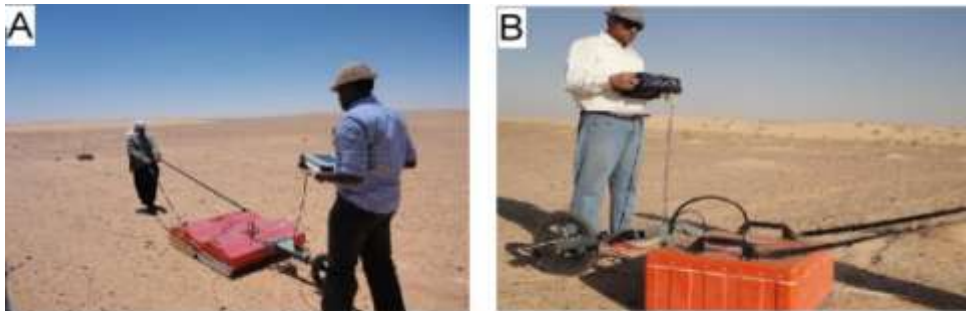


**Figure 5.** A) 100 MHz - Shielded Antenna, and B) 200 MHz - Shielded Antennae. Both were used in the study area.

### 3.2 Multichannel Analysis of Surface Waves (MASW)

The multichannel Analysis of Surface Waves (MASW) is a powerful technique that uses the surface waves for defining subsurface layering, measuring thickness and depth of bedrock. The MASW test is non-invasive, expedient, and cost effective. It can be used to produce a single 1-D VS profile, as well as 2-D VS profile that covers a wide range of area. This means that the 1-D representations of all twenty-seven sites are approximately the same, with few variations in subsurface, which indicates a homogeneous layer of soil. Therefore, the 2-D tomography developed in the study is able to represent both depth and distance. The MASW software will provide high resolution on surfaces that are not weathered, that do not possess excessive reflection areas, and that are of uniform thickness and strength (Anderson, 2010) (see Figure 6).

Twenty-seven surface waves and S-wave profiles surveys were conducted in the study area (see Figure 7). This technique provides a deeper and larger coverage for imaging the subsurface, and for accurately estimating the shear wave velocity of structures more quickly through two-dimensional (1-D, 2-D) tomography of soil layers at depths that are less than or equal to 30 meters (Park et al. 2003). The layout of the MASW method with a faster 2-D tomography technique for subsurface investigations is shown in Figure 5. During data acquisition in applying MASW method, a certain number of receivers (N) were linearly deployed with an even spacing (Dx) over a distance (XT) and a seismic source was located at a certain distance (X0) away from the first receiver. The same source-receiver configuration (SR) was used by following certain interval (dSR) at different locations to acquire multiple records.

The acquisition of the MASW data is relatively straightforward as shown in Figure 5. Twenty-four low-frequency (4.5 Hz) vertical geophones, placed at 1.0 meter intervals, were centered on each test location. Acoustic energy was generated at an offset (distance to the nearest geophone) of 8.0 meters, using an accelerated weight of up to (90.71 kg) 200 lb. The generated Rayleigh waves data were recorded using a 24-channel signal enhancement seismograph, "Strata view" of Geometrics Inc. USA. The acquired Rayleigh wave data was processed using the Kansas Geologic Survey (KGS) software package SurfSeis (Park et al., 2005). This software can process shot records and extract dispersion curves through the initial processing sequences (Ivanov, Park, and Xia 2009). The seismograph recorded the frequency and the travel time of the seismic waves propagating through the subsurface those were later compared with the frequencies measured at particular depth (Anderson, 2010).

The site-specific dispersion curves were generated from field-acquired Rayleigh wave data, and later transformed into vertical shear wave velocity profiles, as shown in Figure 8. The inverted 1-D shear wave velocity profiles reached an average depth of 23 meters. Interpolating and contouring a series of inline 1-D shear wave velocity profiles, results in a 2-D shear wave velocity profile. By incorporating the existing information into 2-D shear wave velocity profiles one could depict the top surface of the bedrock. Processing and analyzing of each acquired multichannel surface wave shot, showed a relatively wide frequency bandwidth reflecting an adequate resolution within a few meters below the ground's surface to a depth of more than 30 meters. Dispersion curve analyses were then performed for each shot gathered and derived from the measurements at twenty-seven core holes by examining the change in phase velocity vs. frequency, by using the fundamental mode component of the dispersion data. Non-linear inversion modeling of each dispersion curve was performed

and resulted in a 1-D mid-point representation of Vs. Interpolation of the 1-D data was done by using a Kriging algorithm which produced a 2-D grid of the Vs data. Color-filled contoured profile plots were then generated from the Vs grid.

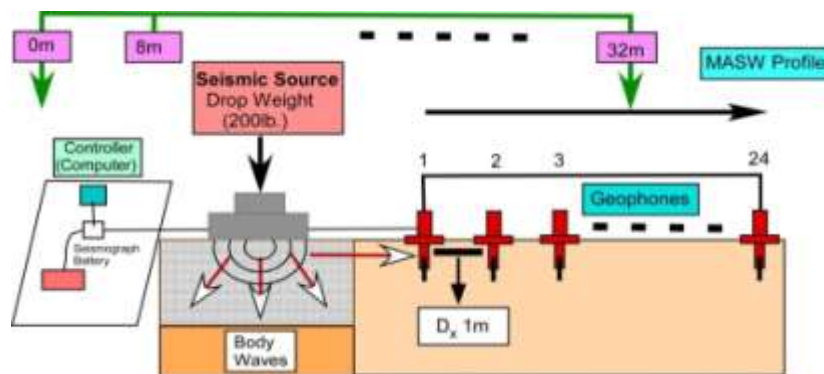


**Figure 6.** Schematic MASW field data acquisition layout, critical factors include; the size of the energy source, the source-receiver offsets, the geophone frequency, the number of geophones, the geophone spacing, and the total array length.

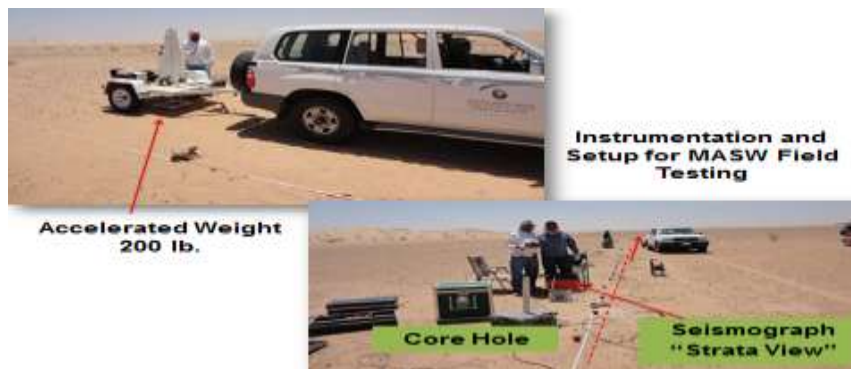


**Figure 7.** Field MASW Survey layout profiling at Dawmat Al Jandal, Al Jawf.

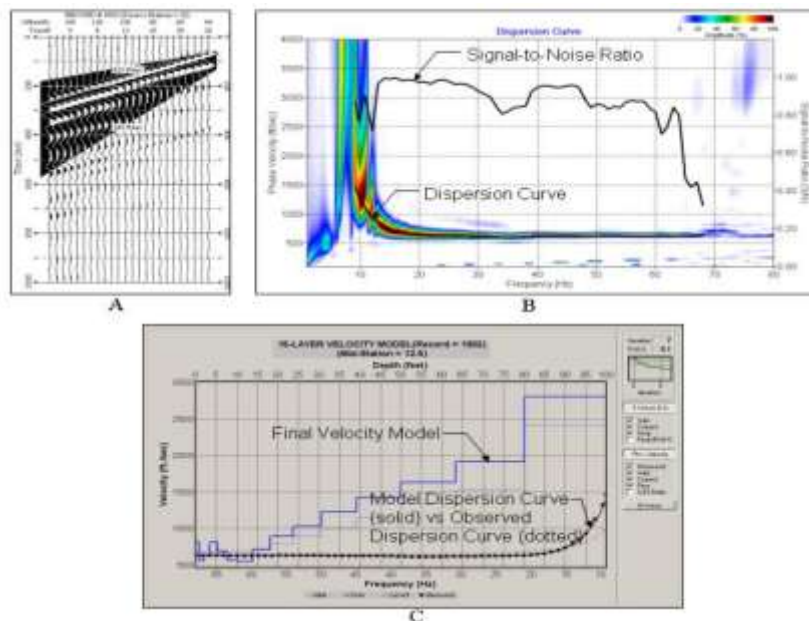


**Figure 8.** Dispersion curves, generated for each acquired Rayleigh wave data set. A) Acquisition seismic time series data, B) Surface wave energy in the frequency domain with the observed dispersion curve was transformed (inversion), and C) shear wave velocity vs inversion model, depth curve.

## IV. RESULTS AND DISCUSSION

### 4.1 Ground Penetrating Radar (GPR)

The accurate interpretation of GPR data is dependent on the nature and appropriateness of data processing. The variation in sediment content often relates to both changes in sediment porosity and permeability, which in turn is dependent on changes in grain size and fabric often associated with lamination, cross-bedding, and bounding surfaces. Emmett et al (1971) observed that porosity and permeability, when parallel to the cross-bed laminate, are higher than when they are perpendicular to the laminate.

There are two major factors that may cause issues when interpreting GPR data: the presence of clay minerals and very inhomogeneous materials. The survey area was found to be very transparent (i.e. clean sands) to GPR signals, and exploration depths in excess of 20 meters were achieved in most of the area. The broad area covered with GPR allowed a clear understanding of the sandy plain area structure.

Two strong reflectors were observed over the area and these were interpreted to be major bounding surfaces. The first major reflector was the chemical analysis of the core holes that confirmed the subsurface deposits of the silica sand. This strong reflector results showed a contrast in the electrical impedance between the silica sand and the quartz-rich sand (SiO<sub>2</sub>) content of 97 percent, iron oxide 0.2 percent, and alumina 1.4 percent.

The second major reflector occurred at the boundary between the layers in the sandy plain area, the outcrops mainly consist of white quartz sand white, and greenish and yellowish sandstone layers. The randomly distributed particle size distributions were composed of fine to medium and coarse grained sands within the sandstone sequence with apparent and frequent graded bedding horizons that indicate multi-sedimentary cycles. Also, joints and fractures without filling materials.

The output data displays the velocity analysis of the radargram obtained along with average thicknesses ranging from 8 to 22 meters. Synthetic hyperbolas with a velocity and the corresponding 2-D ground model for each of the sites were collected along the same survey line over homogeneous silica sand and sand with gravel. The increased shallow resolution for the higher frequencies, offset by the shallower depth of penetration was also evident. The recording time of the two windows in each survey of this study show the number of layers and the depth based on the expected increase, exhaustive of penetration with decreasing dominant frequency. The measurements recorded from 200MHz frequency source, offered the best vertical resolution for up to 8 meters depth, as there was no coherent signal within the deeper portion of the image. Similarly for the 100MHz source, the information was collected beyond 20-22 meters but with the intermediate resolutions. In short the higher frequencies in the 200 MHz image offer the best vertical resolution with up to 8m depth, and the 100MHz image has intermediate resolution with the greater achieved for this study (see Figure 9).

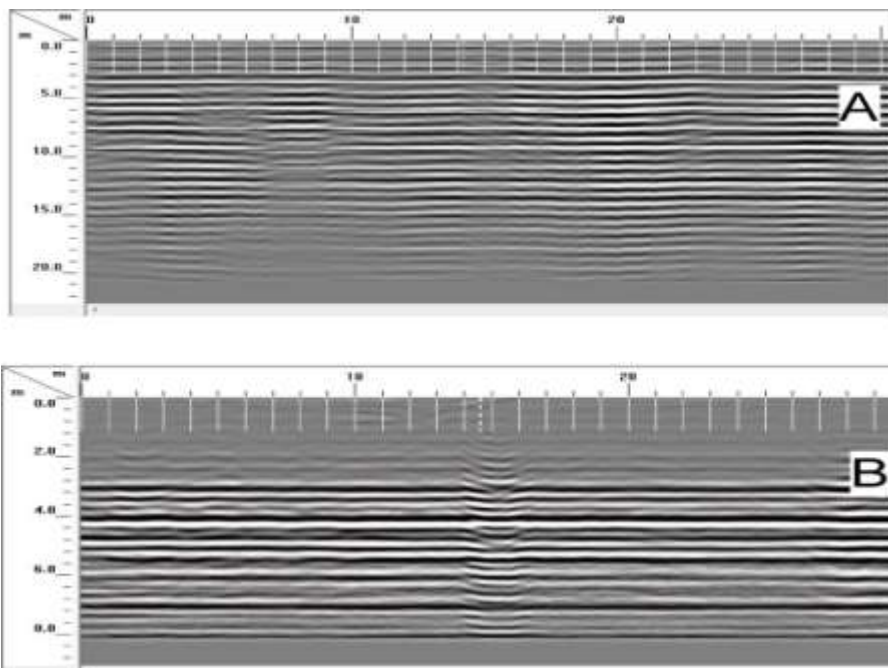


**Figure 9.** Radar profile images along the same survey line for an antennae frequency of, A) 100MHz and, B) 200MHz.

**4.2 Multichannel Analysis of Surface Waves (MASW)**

The results of MASW survey; the number of layers, the S-wave velocities, and the depth. 1-D Velocity models were derived from the dispersion curve, the travel time distance curves, and the corresponding 2-D ground model for each site. They are described based on the “ties” between the 1-D, and 2-D MASW profile and the limited core control (Geo-seismic cross section along profile JSSD-10). Figure 10 shows an example of the depth velocity model of this profile. The interpretation of the shear wave images was carried out to approximate them to be the only layer. The first layer (top layer) identified with velocity ( $V_s$ ) in the range of 400-610 m/s is a friable fine silica sand cover corresponding to a depth about of 35.0 meters, followed by the top of the bedrock at 1-D, 2-D.

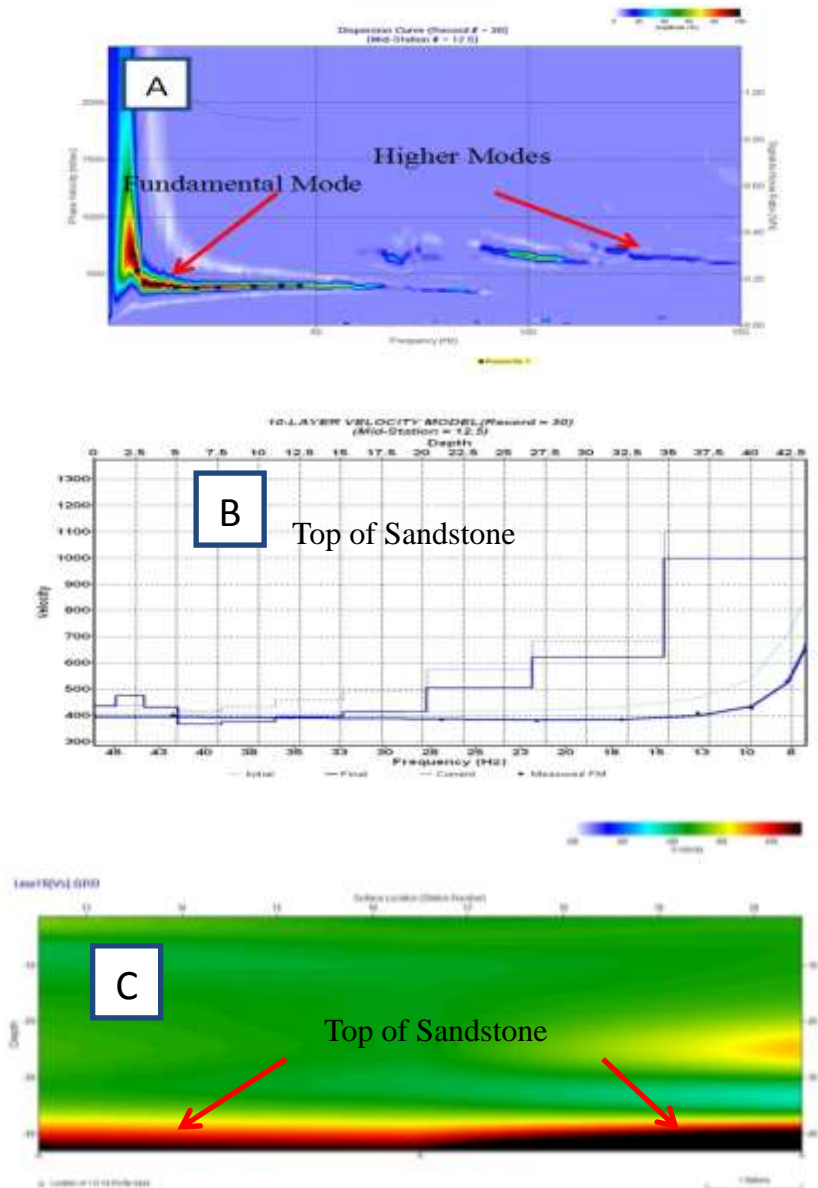


**Figure 10.** JSSD-10: (A) Dispersion Curve, (B) 1-D Shear Wave Velocity, (C) 2-D Shear Wave Velocity Model. (cont.)

Although, Figures (1-D) and (2-D) show 10-layer velocity models, the interpretation of shear wave images were carried out to approximate them s one or two layers. The first layer (top layer) that identified with velocity ( $V_s$ ) in the range of 320-450 m/s is friable fine silica sand with an average thickness from 4 - 23.5 meters. White silica sand was found concentrated, which constitutes the second layer with a velocity ( $V_s$ ) in the range of 450-700 m/s, covering a depth of 16 - 35 meters. In some locations the top of the bedrock was found deeper than 30 meters, and could not be traced. At these locations, the bedrock was presumed to be greater than 30 meters, with a velocity ( $V_s$ ) much greater than 700 m/s. The strong nature of the surface wave energy may be

advantageous when using a simple impact supply, followed by a simple field supply and process. Most significantly the surface waves respond effectively to various types of subsurface deformations that are common targets of geological investigations. Continuous recording of multichannel surface waves shows great promise in mapping the top of the bedrock. Cross sections are generated based on data containing information about the horizontal and vertical continuity of materials, as shallow as a fraction of a meter down to depths of more than 30 meters, depending on the frequency content.

## V. VALIDATION

Twenty-seven core holes with a average depth of 20 m, were drilled in the study area of 20 km<sup>2</sup>. These core holes were drilled perpendicular to the geophysical survey lines in order to compare the survey results. In order to cut short the unnecessary drilling expense the investigation was limited to 20-22m in sands. In most cases the depth of bedrock was not reached.

The basic classification of sandstone and silica / quartz material was performed by chemical analysis on the samples obtained from the field. The analysis showed, the silica contents of the cores are greater than 97 percent (see Table.1). In many industrial applications, the particle size distribution (PSD) of the silica sand is very important. In glass making, the required grain size is between 0.1 and 0.5 mm, or in some cases, 0.1–0.63mm, oversize particles prolong the glass batch melting point while the undersized particles cause air bubbles and weaken the glass products. In the study area the grain size diameter was found between 0.1 to 0.5 mm which best suitable size for glass industry. Overall particle shape of sand grains ranges in the category of sub-rounded to sub-angular with small fraction of rounded particles. There were no true bedding features observed within the sand as all of the samples were characterized as friable fine sand (see Figures 11 & 12).



**Figure 11.** Map Showing the Location of the Core Holes and geophysical at the Silica Sand Deposits in Dawmat Al Jandal Saudi Arabia.



**Figure 12.** Core hole logging of silica sands

The survey area was found to be very transparent (i.e. clean sands) to GPR signals, and exploration depths in excess of 20 meters were achieved in most of the area. The broad area covered with GPR allowed a clear understanding of the sandy plain area structure. Ground truth for the GPR interpretations was obtained by comparing the results with samples representing a total number of twenty-seven core holes. The higher frequencies in the 200 MHz image offer the best vertical resolution with up to 8m depth, and the 100MHz image has intermediate resolution with the greater depth of investigation (nearly 20m for this study).



**Table 1. Log of the Vertical Section.**

**Core hole JSSD – 10**

T.data		Core Recovery	Depth (M)		Description	Log	SiO <sub>2</sub> %			
Depth			%	From				To		
From	To									
0.0	1.50	100	0.0 – 22.70		Light brownish from 0.0 – 0.60 cm after that off white silica sand, fine grain, friable		96.00			
1.50	2.90	100					97.05			
2.90	4.50	100					97.25			
4.50	6.00	100					98.00			
6.00	7.50	100					96.95			
7.50	9.00	100					98.10			
9.00	10.50	100					97.00			
10.50	12.00	100					97.20			
12.00	13.00	100					96.25			
13.00	14.60	100					95.1			
14.60	15.10	100					97.25			
15.10	16.50	100					95.00			
16.50	18.00	100					96.10			
18.00	18.75	100					88.35			
18.75	19.50	100					96.00			
19.50	20.50	100					97.05			
20.50	21.50	100					97.35			
21.50	22.70	100					98.00			
22.70	24.00	100					22.70 – 24.00	Grayish – silica sand, fine grain, friable		96.95

The MASW shear wave velocity values are consistently equal to, or slightly different from, the corresponding core whole values. Differences between the core control downhole and the MASW shear wave velocities may be due to the fact that the MASW velocities are laterally and vertically averaged. Overall, both the core holes and the MASW shear wave velocities’ data compares favorably, which gives confidence in the results of the MASW method of acquiring the data (see Table 2). On average, MASW estimated that the depth to the bedrock at the existing core holes’ locations varies from the core holes’ depths to the top of the bedrock by ~ + 10 (20 meters). The average difference between depths is remarkably small given the variable, the depth to the top of the bedrock, in the study area.

Applying geophysical methods is an excellent alternative to the conventional Core hole methods to provide information in a 1-D or 2-D, easy field acquisition, processing and interpenetrations. Each of these methods has been successful, to varying degrees, in replicating the results obtained by the Core holes’ measurements.

**Table 2.** Acomparison of thickness of Silica sand deposits by the actual core holes measurement and those obtained from the GPR and MASW methods

Line. No	Coordinate		Core hole (m)	GPR	MASW
	Lat N	Long E		Antenna 100MHZ (m)	2-D (m)
JSSD - 1	29 27 17.5	39 51 34.0	18	23.5	22
JSSD - 2	29 28 14.7	39 52 19.0	21.1	21	16
JSSD - 3	29 27 55.6	39 53 30.4	22.7	21	30
JSSD - 4	29 27 40.0	39 54 40.8	17.8	21.5	28
JSSD - 5	29 28 40.8	39 54 58.7	13.7	21.5	30
JSSD - 6	29 28 21.5	39 54 17.6	18.8	21	23
JSSD - 7	29 28 37.3	39 52 57.9	15.6	20.5	30
JSSD - 8	29 29 19.7	39 52 33.0	24.1	21	26
JSSD - 9	29 28 57.2	39 53 43.9	19.7	20	22
JSSD - 10	29 28 58.7	39 54 21.0	24	20.5	35
JSSD - 11	29 29 38.9	39 53 14.2	18.2	20.5	25
JSSD - 12	29 29 51.8	39 52 42.5	19.6	20.5	27
JSSD - 13	29 30 20.1	39 52 49.1	18.2	20	18
JSSD - 14	29 29 19.7	39 55 31.2	19.7	20.5	28
JSSD - 15	29 28 47.9	39 58 34.7	19.7	20	36
JSSD - 16	29 28 28.4	39 59 41.1	19.7	20.5	30
JSSD - 17	29 27 43.5	40 01 10.6	19.7	20	30
JSSD - 18	29 27 50.7	40 00 16.2	19.7	20.5	26
JSSD - 19	29 28 05.8	39 59 07.7	19.7	20.5	30
JSSD - 20	29 27 47.2	39 58 30.5	19.7	20.5	25
JSSD - 21	29 27 29.8	39 59 37.6	19.8	20.5	22
JSSD - 22	29 27 10.4	40 00 48.5	19.8	20	23
JSSD - 23	29 26 31.2	40 00 01.4	19.7	21	25
JSSD - 24	29 26 56.6	39 58 57.6	19.7	20.5	25
JSSD - 25	29 26 44.2	39 58 22.3	17.4	20	28
JSSD - 26	29 25 49.4	39 59 27.1	19.7	20.5	30
JSSD - 27	29 25 14.5	40 00 47.5	19	20.5	29

## VI. CONCLUSIONS

The conclusions of this study are based on field tests conducted on the silica sand deposits, and may not be equally valid at other test sites particularly if the geologic conditions at the other test sites are significantly different. It was not required to access the top of the bedrock due to the high cost of drilling and the believing that the current depth of investigation is sufficient for the study and there were no isolated bedding features observed within the entire sand deposit that confirm as this friable fine sand. The results of this study (the geophysical site investigation performed using GPR and MASW methods) were validated from the core hole results.

The use of GPR was found very effective because of the rapid profiling and initial interpretations with minimal data processing for shallow geophysical investigation (i.e. to estimate thickness of sand depths up to 20m). The GPR depth of penetration is limited compared with the MASW method, but it is more effective to map bedding planes within sand, dry, sandy to seeing the space between layers to better understand depositional environment. A fairly good correlation between the radar and the geological section was observed, especially the results obtained from using the lower frequency antenna (100 MHz shielded GPR), that clearly displays the subsurface layered sands upto 20 meters depths. Thus, it was able to recognize areas of a succession of silica sand, sand layers, and places that are made up of areas with no obvious surface layer.

The MASW velocity profile shows excellent agreement with the core holes' measurements. The comparison of MASW-estimated bedrock depths and proximal ground truth (core holes sites) are equal to, or slightly different from, the corresponding core holes' downhole values.

Overall, both the Core holes and the MASW shear wave velocities' data compares favorably, which gives confidence of the MASW method. The author believes also that the differences in the depths are due to the geophysical possibilities, to penetration, or to topographic variation of the subsurface. So, there are areas of low velocity and low density that correspond with the subsurface structure, such as the depth of the silica sand about the top of the bedrock or sandstone.

This study clearly indicates the usefulness of both of the applied geophysical methods in investigating the thickness of silica sand deposits in the vicinity of Dawmat Al Jandal, Al Jawf in Saudi Arabia. The study also reduced the drilling cost remarkably as results of these surveys showed satisfactory correlations between the estimated and actual values.

## REFERENCES

- [1]. Anderson, N. (2010). Lectures in: Ground Penetrating Radar Applications in Engineering and Environmental Studies. GE482. Rolla, Missouri, USA: Missouri University of Science and Technology
- [2]. Annan, A.P., 2002. GPR – History, Trends, and Future Developments. *Subsurface Sensing Technologies and Applications* 3 (4), 253 – 270.
- [3]. Bramkamp, R.A., Ramirez, L.F., Seineke, M and Reiss, W.H., 1963, Geology of the Jawf-Sakakah quadrangle, Kingdom of Saudi Arabia: Geological Survey Saudi Arabian Mission Miscellaneous Geologic Investigations Map I-201A, scale 1:500,000.
- [4]. Burger, H. Robert, Sheehan, Anne F., and Jones, Craig H., 2006. *Introduction to Applied Geophysics : Exploring the Shallow Subsurface*. New York: W.W. Norton. ISBN 0-393-92637-0.
- [5]. Cassidy, N. J., 2009. *Electrical and Magnetic Properties of Rocks, Soils and Fluids*. In H. Jol (Ed.), *Ground Penetrating Radar: Theory and Applications* (pp. 41-72). Solvenia: Elsevier B. V.
- [6]. Cassidy, N. J. (2009b). *Ground Penetrating Radar Data Processing, Modeling and Analysis*. In H. Jol (Ed.), *Ground Penetrating Radar: Theory and Applications* (pp. 141-176). Solvenia: Elsevier B. V.
- [7]. Emmett, W. R., K. W. Beaver, and J. A. McCaleb, 1971, Little Buffalo Basin Tensleep heterogeneity – its influence on infilling drilling and secondary recovery. *Journal of Petroleum Technology*, p. 161-168.
- [8]. Ghandoura, R.A., Al-Nakhebi, Z.A., Tayeb, O.M., Al-Tamimi, M.A., and Al-Sulimani, G., 2012. Detailed study on Dawmat Al Jandal silica sand, Al Jawf region, Kingdom of Saudi Arabia: Saudi Geological Survey Technical Report SGS-TR-2011-8, 23p.
- [9]. GSSI SIR-3000 User's Manual. Salem, New Hampshire: Geophysical System Survey Inc 2006. Bridge Assessment Module: RADAN 6.5 User's Manual MN 43-172 Rev C. Salem New Hampshire: Geophysical Survey Inc. 2007.
- [10]. Ivanov, Julian, Choon Park, and Jianghai Xia. "MASW/SurfSeis 2 Workshop." Fort Worth: Kansas Geologic Survey, March 28, 2009.
- [11]. Jol, H. M., and Smith, D. G., 1991. Ground penetrating radar of northern lacustrine deltas. *Canadian Journal of Earth Sciences*, 28, pp. 1939-1947.
- [12]. Pellerin L., 2002. *Applications of Electrical and Electromagnetic Methods for Environmental and Geotechnical Investigations Surveys in Geophysics*, 23, pp. 101-132.

- [13]. Kovic, O., & Anderson, N. 2005. Use of Ground Penetrating Radar for Fracture Imaging. Applied Geophysics Conference, pp. 566-573.
- [14]. Reynolds, J.M., 1997. An introduction to applied and environmental geophysics, John Wiley & Sons Ltd., West Sussex, England.
- [15]. Park, Choon, B, Richard D Miller, JianghiXia, and Julian Ivanov, 2000. Multichannel Seismic Surface-Wave Methods for Geotechnical Applications. First International Conference on the Application of Geophysical Methodologies to Transportation Facilities and Infrastructure. St. Louis.
- [16]. Park, Choon B., 2005. MASW Horizontal Resolution in 2D Shear-Velocity ( $V_s$ ) Mapping. Open-File Report, Lawrence: Kansas Geologic Survey.
- [17]. Park, Choon B, Richard Miller, Jianghai Xia, Nils Ryden, and Peter Ulriksen. 2003. The MASW Method - What and Where it is." EAGE 65th Conference and Exhibition. Stavanger.
- [18]. Park, C B, Miller R D and Xia, J., 1999. Multichannel analysis of surface waves, Geophysics 64, pp. 800-808.
- [19]. Surf-Seis. Multi Channel Analysis of Surface Waves. 2006. Retrieved February 3, 2010 from: <http://www.kgs.ku.edu/software/surfseis/masw.html>
- [20]. Xia, J., Miller, R. D., Park, C. B., and Ivanov, J., 2001. Feasibility of determining  $Q$  of near-surface materials from Rayleigh waves: [Exp. Abs.]: Soc. Expl. Geophys, pp. 1381-1384.
- [21]. Xia, J., Miller, R. D., and Park, C. B., 1999, Estimation of near-surface shear wave velocity by inversion of Rayleigh waves: Geophysics, 64, pp. 691-700.